

Accepted Manuscript

Geochronology and landscape evolution of the strand-plain of the Usumacinta and Grijalva rivers, southern Mexico

Esperanza Muñoz-Salinas, Miguel Castillo, David Sanderson, Tim Kinnaird



PII: S0895-9811(17)30269-9

DOI: [10.1016/j.jsames.2017.08.021](https://doi.org/10.1016/j.jsames.2017.08.021)

Reference: SAMES 1762

To appear in: *Journal of South American Earth Sciences*

Received Date: 3 July 2017

Revised Date: 25 August 2017

Accepted Date: 28 August 2017

Please cite this article as: Muñoz-Salinas, E., Castillo, M., Sanderson, D., Kinnaird, T., Geochronology and landscape evolution of the strand-plain of the Usumacinta and Grijalva rivers, southern Mexico, *Journal of South American Earth Sciences* (2017), doi: 10.1016/j.jsames.2017.08.021.

This is a PDF file of an unedited manuscript that has been accepted for publication. As a service to our customers we are providing this early version of the manuscript. The manuscript will undergo copyediting, typesetting, and review of the resulting proof before it is published in its final form. Please note that during the production process errors may be discovered which could affect the content, and all legal disclaimers that apply to the journal pertain.

1 **Geochronology and landscape evolution of the strand-plain of**
2 **the Usumacinta and Grijalva rivers, southern Mexico**

3
4 **Esperanza Muñoz-Salinas^{1,*}, Miguel Castillo², David Sanderson³, Tim Kinnaird⁴**

5
6 ¹Instituto de Geología, Universidad Nacional Autónoma de México, UNAM, Ciudad
7 Universitaria 3000, P.C. 02510, Mexico City, Mexico. Email: Esperanzam@ownmail.net,
8 telephone: +52 (55) (525) 622 4300 Ext. 109

9
10 ²Instituto de Geología, Universidad Nacional Autónoma de México, UNAM, Ciudad
11 Universitaria 3000, P.C. 02510, Mexico City, Mexico. Email:
12 Castillom@geologia.unam.mx, telephone: +52 (55) 56224288 Ext. 241

13
14 ³Scottish Universities Environmental Research Centre, SUERC, Rankine Avenue, Scottish
15 Enterprise Technology Park, East Kilbride, G75 0QF, Glasgow, UK. Email:
16 David.Sanderson@glasgow.ac.uk, telephone: (+33) 01355270110

17

18 ⁴Earth and Environmental Sciences Department, School of Earth and Environmental
19 Sciences, University of St Andrews, Irvine building, St Andrews, UK. Email: tk17@st-
20 andrews.ac.uk, telephone: (+33) 01334463911

21 *Corresponding author

22

23

24 **Abstract**

25

26 The strand-plain of the Usumacinta and Grijalva rivers is the largest of the Gulf of Mexico
27 as it is characterized by a sequence of well-preserved beach-dune ridges ($n > 100$)
28 distributed ~150 km along the shoreline. This prominent coastal landform is part of the
29 delta plain of Tabasco and Campeche. We present geochronological data of the beach-dune
30 ridges sequence of the Usumacinta and Grijalva rivers. Radiocarbon dating failed in
31 providing consistent ages of the ridges in contrast to optically stimulated luminescence
32 (OSL), which yielded coherent and robust dates. The oldest beach-dune ridges were formed
33 ~2.5 ka. The presence of blocked-valley lakes evidences a recent process of sediment
34 aggradation on the delta plain caused by a marine transgression. Using a regression model
35 with the OSL ages and the distance of beach-dune ridges from the shoreline we estimate

36 that the autoretreat yielded the sediment accumulation ~ 7 ka. Our estimation agrees with
37 other general models of sea level rising in the Gulf of Mexico that consider a marine
38 stabilization initiated about ~ 6 to 7 ka. The progradation rates of the beach-dune ridges (4.7
39 to 8.9 m yr⁻¹) place this strand-plain among those with high sedimentation rates in the Gulf
40 of Mexico and, perhaps, around the world.

41

42 **Keywords**

43 Strand-plain of Usumacinta and Grijalva rivers, delta plain of Tabasco and Campeche,
44 landscape evolution, OSL, Gulf of Mexico

45

46 **1. Introduction**

47 Strand-plains are present in all continents but they are more frequent in wave-dominated
48 beaches where there is a large amount of terrigenous sediment in the foreshore that is
49 delivered by rivers (Nordstrom et al., 1991; Otvos, 2000; Tamura, 2012). This type of
50 landform is composed of beach-dune ridges sequences that form in decadal time-scales and
51 prograde toward the sea. In cases where the geochronology of ridges is well constrained
52 the progradational rates are established using the distance of the ridges from inland to the
53 sea. In the Gulf of Mexico, the progradational rates for strand-plains range from 0.08 m yr⁻¹

54 in the Apalachicola Barrier (Rink and López, 2010) to 1.57 m yr^{-1} for Merrit Island in
55 Florida (Rink and Forrest, 2005). For other strand-plains around the world, low
56 progradational rates have been reported in SW Australia, with 0.57 m yr^{-1} in the coast of
57 New South Wales (Thom et al., 1978) and 0.38 m yr^{-1} in Guichen Bay, south Australia
58 (Murray-Wallace et al., 2002); moderate progradational rates in Phra Thong Island, in
59 Thailand, with 2.7 m yr^{-1} (Brill et al., 2012); and higher rates in Skalligen Spit in Denmark
60 with 30 m yr^{-1} (Aagaard et al., 2007).

61

62 We investigate the strand-plain of the Usumacinta and Grijalva rivers (southern Mexico)
63 which forms part of a large delta plain (Fig. 1). The Usumacinta-Grijalva strand-plain is
64 the largest of the Gulf of Mexico as $\sim 150 \text{ km}$ wide, that includes part of the coast of
65 Tabasco and Campeche and extends for more than 25 km inland. This landscape preserves
66 more than 100 beach-dune ridges, and constitutes a unique sedimentary record for
67 understanding the sedimentation rates of the coastal plain of Tabasco and Campeche, and
68 denudation rates for the highlands of southern Mexico and northern Guatemala. Moreover,
69 the strand-plain is also direct evidence for the evolution of the Usumacinta and Grijalva
70 rivers, which together form a river system ranked in the 10th position of the largest rivers of

71 North America with a mean annual discharge of $\sim 2,678 \text{ m}^3 \text{ s}^{-1}$ (Hudson et al., 2005; Benke,
72 2009).

73

74 Despite its extension and geological significance, the region has remained largely
75 understudied (Davis, 2011). Psuty (1965; 1967) and West et al. (1969) conducted the
76 pioneering study of this strand-plain in the 1960s. Based on the projection of the subparallel
77 beach-dune ridges toward the sea, they recognized three progradational phases associated
78 with the relocation of the mouth of the Usumacinta and Grijalva rivers. They, however, did
79 not provide ages of the strand-plain and they only considered the strand-plain as recent
80 fluvial feature of the Quaternary. More recently, Hernández Santana et al., (2007)
81 delineated the translocation of the shoreline of the coasts of Tabasco and Campeche based
82 on the interpretation of aerial photographs.

83

84 Our main goal is to provide a robust dating of the beach-dune ridges of this strand-plain to
85 tease out the different phases of its evolution. For this purpose, we use Accelerator Mass
86 Spectrometry (AMS) ^{14}C and Optically Stimulated Luminescence (OSL) analysis. OSL has
87 been proved to provide accurate dates of strand-plain deposits because these tend to be
88 well-reset due to the aeolian redistribution of sediment during the beach-dunes formation

89 (Rink and Pieper, 2001; Rink, 2003). The role of aeolian processes in the formation of
90 beach-dune ridges among different strand-plains around the world is under debate (Tamura,
91 2012), however, the studies of Psuty (1965; 1967) and West et al. (1969) indicate that
92 aeolian processes are important in the formation of beach-dune ridges in the coast of
93 Tabasco and Campeche. They observed that the sand transported to the beach by middle
94 intensity waves is redeposited to the top of berms by winds (Psuty, 1965; 1967).

95

96 **2. Methods**

97 2.1. *Radiocarbon and OSL analysis*

98 In November 2015, fieldwork was undertaken in Tabasco and Campeche to extract the
99 samples from different beach-dune ridges on the strand-plain for dating. Our sampling
100 strategy consisted of collecting samples from along two transects perpendicular to the
101 coast. We carefully selected only those lands with undisturbed beach-dune ridges and
102 avoided in all cases those sites with evidences of anthropic perturbation. We sampled eight
103 sites with well-preserved crests around the strand-plain of Usumacinta and Grijalva rivers
104 (Figs. 2 and 3).

105

106 To extract samples for OSL and AMS ^{14}C dating we excavated a hole in the top of crests.
107 We covered the hole with a black opaque blanket and we took samples at ~0.5 m of depth
108 by inserting a plastic tube of 20 cm long and 5 cm diameter into the deposit. Once the tube
109 was filled with sediment, we extracted and covered it with aluminum foil. The sampled
110 material was used for both luminescence analysis and determination of the environmental
111 dose rates in the laboratory. We removed the sediment adjacent to the place where we
112 extracted the tube and collected ~500 g of material in a bag that was used in the laboratory
113 for the determination of the gamma dose rates. These samples were analyzed at the Scottish
114 Environmental Research Centre (SUERC), in the United Kingdom, using the single aliquot
115 regenerative (SAR) method on grains of quartz. For radiocarbon analysis, we extracted
116 chunks of organic matter, charcoal and organic sediment from inside the same holes from
117 the same ridge where we extracted the OSL samples. Four of the samples were sent to the
118 Beta Analytic Laboratory in USA for their analysis with an AMS.

119

120 *2.2. Terrain analysis*

121 We used Landsat 8 images and ASTER digital elevation models (DEMs) of 30 m
122 resolution for photointerpretation of major phases of evolution of the Usumacinta and
123 Grijalva strand-plain. Both products were downloaded from the USGS webpage

124 (<https://landsat.usgs.gov>). We also analyzed the available high-resolution digital elevation
125 models (HRDEM) of 3 m of resolution from LIDAR datasets offered by the INEGI in their
126 webpage (<http://www.inegi.org.mx>) which was manipulated in Arc Gis10.1.

127

128

129 **3. Results and discussion**

130 *3.1 Phases of evolution of the strand-plain of the Usumacinta and Grijalva rivers*
131 *according to photointerpretation*

132

133 The three progradational phases of evolution of the strand-plain identified by Psuty (1965;
134 1967) and West et al. (1969) were confirmed based on photointerpretation of Landsat 8
135 images and ASTER digital elevation models (DEMs) of 30 m resolution.

136

137 During phase I the Usumacinta and Grijalva rivers flowed separately into the Gulf of
138 Mexico. The evidence of this formative period is in the western sector of the strand-plain
139 where the beach-dune ridges are oriented from NW to SE (Fig. 2). The NW-SE orientation
140 indicates that a river inlet flowed ~10 km west from Grijalva River current position. The
141 Grijalva River migrated toward the east in previous episodes to the phase I. This is

142 confirmed by the presence of palaeo-channels along the coastal plain of Tabasco and the
143 eroded beach-dune ridges found in the river mouth of Tonala and Rio Seco rivers (Fig.1B).
144 During this phase the Usumacinta River probably discharged into the sea, near to Laguna
145 de Terminos (Fig. 1).

146

147 During phase II the orientation of the beach-dune ridges indicates that the Usumacinta and
148 Grijalva rivers joined a few kilometers inland and flowed into the sea through the San
149 Pedro-San Pablo (SPSP) River (Fig. 2). Projecting this set of beach-dune ridges toward the
150 sea, we reconstructed a delta lobe that protruded ~6 km seaward. In this phase, a palaeo-
151 channel in the western sector of the strand-plain evolved contemporaneously with the delta
152 lobe at the SPSP River. This palaeo-channel has a distributary channel that was created
153 when the Grijalva River flowed into the sea during phase I and it incises part of the beach-
154 dune ridges built in the phase II.

155

156 Phase III initiated with the migration of Usumacinta and Grijalva rivers toward the west
157 where they have remained in their current position (Fig. 2). In this phase these rivers have
158 built the modern delta lobe. In this phase the SPSP River dropped its rate of sediment
159 delivered to the sea and the sea waves started to erode the delta lobe formed during phase II

160 (see Fig. 4). The precise timing when phase II changed to phase III is when the modern
161 delta lobe grew up and the old delta lobe at SPSP River started to be eroded.

162

163 3.2. OSL and Radiocarbon results

164 Radiocarbon samples resulted in very young ages ranging from 233 ± 236 BP to post 0 BP.

165 The sample extracted close to the shoreline provided post 0 BP, in the middle part of the
166 strand-plain, the closer sample to the coast is of 180 ± 44 BP and the farther inland of $233 \pm$

167 236 BP. The sample located in the furthest point inland yield an age of post 0 BP. Three of

168 the four AMS ^{14}C dates contain younger dates toward the shoreline but the sample located

169 farther inland yield a post 0 BP age (see Table 1). All the AMS ^{14}C dates are yielding very

170 recent ages making difficult to constrain the age of strand-plain. We interpreted that the

171 ages are indicative of the colonization of vegetal species on the strand-plain rather than the

172 beach-dune ridges formation.

173

174 OSL ages ranged from 560 ± 40 BC (2.57 ± 0.04 ka) in the ridge sampled farther inland to

175 1880 ± 5 AD (0.14 ± 0.01 ka) for the sample extracted close the shoreline and in the current

176 delta lobe. We observed a strong linear correlation between OSL ages versus their distance

177 from the shoreline ($R^2 = 0.88$; $p < 0.01$; $F < 0.01$) (Fig. 2 and Table 2). This trend agrees with

178 a simple progradational sequence model of deposits. OSL ages are within historical time,
179 spanning through the Middle and Late Preclassic, and the Classic periods of the Maya
180 chronology (Mascarelli, 2010).

181

182 *3.3. Contrasting OSL results with historical records*

183

184 OSL ages suggest that the strand-plain of the Usumacinta and Grijalva rivers was under
185 formation during the time of the Maya Civilization apogee. The spatial distribution of the
186 Maya archeological sites in Tabasco and Campeche are located outside the strand-plain of
187 the Usumacinta and Grijalva rivers (see Fig. 1). Although this fact does not prove by itself
188 that the strand-plain was under sedimentation during the time of the Maya Civilization, the
189 lack of evidences of human occupation in the strand-plain supports the fact that this
190 landform was in formation during that time.

191

192 The first historical record of the Usumacinta and Grijalva rivers area is from the writings of
193 the Spanish Armada that arrived to the southern coasts of the Gulf of Mexico in 1518 AD
194 [García-Icazbalceta, 1972]. These documents described how the ship of Juan de Grijalva
195 navigated the mouth of the Usumacinta and Grijalva rivers. This historical evidence

196 indicates that in 1518 AD the strand-plain was in phase III of evolution. We used the age
197 of samples D6 and D8 to calculate the time of transition between phases II and III,
198 assuming a constant progradational rate. The distance between samples is 5.5 km, and the
199 transition between phase II to III occurred ~4.5 km seaward from sample D8. Using the
200 progradational rate model of 0.87 m y^{-1} we calculated that the transition between phase II
201 and III, that is also the starting date of phase III occurred ~1383 AD. This date agrees with
202 the fact that in 1510 AD, when Juan de Grijalva arrived to the coasts of Tabasco and
203 Campeche, the strand-plain was on its phase III of evolution.

204

205 Projecting the orientation of the truncated beach-dune ridges of the delta lobe of the SPSP
206 River (phase II) we estimated the mean erosion rate on this delta lobe, constraining the date
207 for transition between phases II and III at 1405 AD. The mean erosion rate was 10 m yr^{-1} .
208 Hernández Santana et al (2007) calculated a mean erosion rate of 8 m yr^{-1} in this same delta
209 lobe between 1943 to 1995 by using aerial photographs of the coasts of Campeche and
210 Tabasco. In this case, this independent study agrees with our estimation of the erosion rates
211 for the delta lobe of the SPSP River using the OSL ages.

212

213 *3.4.Landscape evolution of the strand-plain of the Usumacinta and Grijalva rivers*
214 *according to OSL ages*

215

216 Our regression model demonstrates that there is a linear relationship between distance from
217 the shoreline and age of the sampled sites (Fig. 2). All the ages prograde towards the coast
218 with exception of sample D2 (2.57 ± 0.04 ka) that is in phase II but is older than D1 (Table
219 2). Because D2 is very close to a paleo-channel (Fig. 2) we suspect that partially bleached
220 grains transported in this fluvial environment were deposited on the top of the ridge at the
221 time the paleo-channel was active. Thus, the OSL age of D2 yields an older age than it
222 should be according to its position in the strand-plain.

223

224 Using the OSL ages we propose that phase I of evolution of the strand-plain initiated ~ 2.5
225 ka, as the sample located farther inland, D1, yielded 2.37 ± 0.07 ka. To calculate the
226 beginning of Phase II, we considered that the first beach-dune ridge was located at ~ 1 km
227 inland from D8. Using the same progradational model of 0.87 m y^{-1} used to estimate the
228 beginning of Phase III, we calculated that Phase II initiated ~ 1.25 ka by adding 113 years to
229 the age of D8 (1.14 ± 0.03 ka). As mentioned above, Phase III initiated ~ 0.63 ka (i.e. 1383
230 BC).

231

232 The progradation rates in the strand-plain variate among the different OSL samples
233 between 4.7 to 8.9 m yr⁻¹ and a mean period of bar formation of 13.5 m/yr. These values
234 place the strand-plain of the Usumacinta and Grijalva rivers among those with high
235 sedimentation rates in the Gulf of Mexico and around the world (Fig. 5).

236

237 *3.5. The strand-plain of the Usumacinta and Grijalva rivers in the delta plain of the*
238 *Tabasco and Campeche*

239

240 We recognized two sectors of the delta plain: (1) the western sector, which is composed by
241 abandoned river channels and some remnants of eroded beach-dune ridges sequences
242 located along the shoreline (Fig. 1B) and (2) the eastern sector, which contains the strand-
243 plain of the Usumacinta and Grijalva rivers and where the current channels of these rivers
244 distribute and flow into the sea (Fig. 1B). The western sector has a lower elevation than the
245 eastern sector (Fig. 1), supporting our interpretation that the sedimentation rates in the delta
246 plain are higher in the east.

247

248 The boundary between the delta plain and the sierra that is marked by an abrupt change in
249 elevation at an average distance from the current shoreline of 90 km, characterized by the
250 presence of blocked-valley lakes, particularly in the eastern sector (Fig. 1). These kinds of
251 lakes indicate that a process of sediment aggradation dammed valleys with insufficient
252 discharge to incise into the coastal plain, like in the case of some tributaries of the Fly River
253 in Papua New Guinea (Lauer et al., 2008). The aggradation process of the delta plain
254 suggests that a marine transgression inundated the surface, more recently in the eastern part
255 of the delta which has a lower elevation, and it was followed by a process of sediment
256 accumulation initiated in the boundary between the delta plain and the sierra and
257 progressively moving towards the sea (Muto and Steel, 1997; Canestrelli et al., 2010).
258 Therefore, the strand-plain of the Usumacinta and Grijalva rivers, that occupies ~25% of
259 the southern sector of the delta plain, correspond to the youngest feature only. To calculate
260 the moment in which the deltaic autoretreat stopped and started the sediment accumulation
261 in the delta, we used a regression model of the OSL ages to distance to the shoreline. For
262 this purpose, we assumed that the sediment delivery from the Usumacinta and Grijalva
263 rivers has remained constant. We obtained that the model of aggradation of the eastern
264 sector delta plain occurred ~7 ka (Fig. 2). Considering that the sea-level rise started to
265 cease about ~6 ka time in the Gulf of Mexico (Balsillie and Donoghue, 2004), our

266 estimation of the formation of the delta is plausible. Finally, we propose that after the
267 marine transgression, the sediment accommodation in the southern sector of the delta plain
268 must have initiated under shallow waters that inhibited beach-dune ridge formation; as the
269 intensity of waves should have been reduced. When the shoreline moved toward deeper
270 waters, wave energy increased enough to form beach-dune ridges. This explains the lack of
271 beach-dune ridges in the inland part of the delta plain.

272

273 **4. Conclusions**

274 We introduce a robust geochronological record of the largest strand-plain of the Gulf of
275 Mexico and one of the most important worldwide. Eight OSL ages allow us to constrain the
276 different phases of evolution of the strand-plain of the Usumacinta and Grijalva rivers and
277 to provide progradation rates during its formation. Based on a regression model between
278 OSL ages and distance we propose that aggradation in the coastal plain of Tabasco and
279 Campeche initiated ~7 ka by the onset of sea-level stabilization on the Gulf of Mexico.
280 Results of this study strongly suggest that the strand-plain of the Usumacinta and Grijalva
281 rivers is among the highest denudational rates reported for the Gulf of Mexico and among
282 the world.

283

284 **Acknowledgements**

285 Fieldwork and OSL laboratory analysis were funded by the project UNAM-PAPIIT
286 (IA102615). We thank Dr. Correa-Metrio and an anonymous reviewer for their thoughtful
287 comments which improved the final version of the manuscript.

288

289 **References**

290

291 Aagaard, T.J., Orford, J., Murray, A.S., 2007. Environmental controls on coastal dune
292 formation: Skallingen Spit, Denmark. *Geomorphology*, 83, 29-47.

293

294 Argyilan, E.P., Forman, S.L., Johnston, J.W., Wilcox, D.A., 2005. Optically stimulated
295 luminescence dating of late Holocene raised strandplain sequences adjacent to Lakes
296 Michigan and Superior, Upper Peninsula, Michigan, USA. *Quaternary Research*, 63, 122-
297 135.

298

299 Balsillie, J.H., Donoghue, J.F., 2004. High resolution sea-level history for the Gulf of
300 Mexico since the last glacial maximum. Florida Geological Survey Report of
301 Investigations. Tallahassee: Florida.

302

303 Benke, A.C., 2009. Streams and Rivers of North America: Western, Northern and Mexican
304 Basins, in: Benke, A.C., Cushing, C.E. (Eds.), Northern and Mexican Basins in
305 Encyclopedia of Inland Waters: Elsevier.

306

307 Blaauw, M. 2010. Methods and code for “classical” age-modelling of radiocarbon
308 sequences. Quaternary Geochronology, 5, 512-518.

309

310 Brill, D., Klasen, N., Brueckner, H., Jankaew, K., Scheffers, A., Kelletat, D, Scheffers, S.,
311 2012. OSL dating of tsunami deposits from Phra Thong Island, Thailand. Quaternary
312 Geochronology, 10, 224-229.

313

314 Canestrelli, A. S., Fagherazzi, A., Defina, S., Lanzoni, S., 2010. Tidal hydrodynamics and
315 erosional power in the Fly River delta, Papua New Guinea. Journal of Geophysical
316 Research, 115, F04033.

317

318 Davis, R.A., 2011. Sea-level change in the Gulf of Mexico. Texas A&M University Press.

319

320 García-Icazbalceta, J., 1972. Itinerario de la armada del Rey Católico a la Isla de Yucatán
321 en la India, el año 1518 en la que fue por comandante y capitán general Juan de Grijalva.
322 Escrito para su alteza por el capellán mayor de dicha armada. Juan Pablos: Mexico.

323

324 Hernández Santana, J.R., Ortiz Pérez, M.A., Méndez Linares, A.P., Gama Campillo, L.,
325 2007. Morfodinámica de la línea de costa del estado de Tabasco, México: tendencias desde
326 la segunda mitad del siglo XX hasta el presente. Investigaciones geográficas, Boletín del
327 Instituto de Geografía, 65, 7-21.

328

329 Hudson, P., Hendrickson, D., Benke, A.C., Varela-Romero, A., Rodiles-Hernández, R.,
330 Minckley, W.L., 2005. Rivers of Mexico, in: Benke, A.C. and Cushing, C.E. (Eds.), Rivers
331 of North America. Academic Press: California.

332

333 Kinnaird, T.C., Sanderson, D.C.W., Muñoz-Salinas, E., Castillo, M., 2016. Delta
334 switching: evolution of the Usumacinta-Grijalva and San Pedro deltas. OSL dating report,
335 SUERC.

336

337 Mascarelli, A. 2010. Mayans converted wetlands to farmland. *Nature news*,
338 doi:10.1038/news.2010.587

339

340 Mejdahl, V., 1979. Thermoluminescence dating: Beta-dose attenuation in quartz grains.
341 *Archaeometry*, 21, 61-72.

342

343 Murray, A.S., Wintle, A.G., 2000. Luminescence dating of quartz using an improved
344 single-aliquot regenerative-dose protocol. *Radiation Measurements*, 32, 57-73.

345

346 Murray-Wallace, C.V., Banerjee, D., Bourman, R.P., Olley, J.M., Brooke, B.P., 2002.
347 Optically stimulated luminescence dating of Holocene relict foredunes, Guichen Bay, South
348 Australia. *Quaternary Science Reviews*, 21, 1077-1086.

349 Muto, T., Steel, R.J., 1997. Principles of regression and transgression: The nature of the
350 interplay between accommodation and sediment supply. *Journal of Sedimentary Research*,
351 67, 994-1000.

352 Nordstrom, K., Psuty, N., Carter, B., 1991. Coastal dunes: Form and process. John Wiley
353 and sons.

354

355 Otvos, E.G., 2000. Beach ridges – definitions and significance. *Geomorphology*, 32, 83-
356 1008.

357

358 Prescott, J.R., Hutton, J.T., 1994. Cosmic ray contributions to dose rates for luminescence
359 and ESR dating: Large depths and long-term time variations. *Radiation Measurements*, 23,
360 497-500.

361

362 Psuty, N.P., 1965. Beach-ridge development in Tabasco, Mexico. *Annals Association of*
363 *American Geographers*, 55, 112-124.

364

365 Psuty, N.P., 1967. The geomorphology of beach-ridges in Tabasco, Mexico. Louisiana
366 State University Coastal Studies Institution Technical Report n° 30.

367

368 R Development Core Team, 2009. R: A language and environment for statistical
369 computing: R foundation for Statistical Computing, <http://www.r-project.org>.

370

371 Reimer, P.J., Bard, E., Bayliss, A., Beck, J.W., 2013. IntCal13 and Marine13 radiocarbon
372 age calibration curves, 0-50,000 years cal BP. *Radiocarbon*, 55, 1869-1887.

373

374 Rink, W.J., Pieper, K.D., 2001. Quartz thermoluminescence in a storm deposit and a
375 welded beach ridge. *Quaternary Science Reviews*, 20, 815-820.

376

377 Rink, W.J., 2003. Thermoluminescence of Quartz and Feldspar Sand Grains as a Tracer of
378 Nearshore Environmental Processes in the Southeastern Mediterranean Sea. *Journal of*
379 *Coastal Research*, 19, 723-730.

380

381 Rink, W.J., Forrest, B., 2005. Dating Evidence for the Accretion History of Beach Ridges
382 on Cape Canaveral and Merrit Island, Florida, USA. *Journal of Coastal Research*, 21, 1000-
383 1009.

384

385 Rink, W.J., López, G.I., 2010. OSL-based lateral progradation and Aeolian sediment
386 accumulation rates for the Apalachicola Barrier Island Complex, North Gulf of Mexico,
387 Florida. *Geomorphology*, 123, 330-342.

388

389 Sanderson, D., 1988. Thick source beta counting (TSBC): A rapid method for measuring
390 beta dose-rates. *International of Radiation Applications and Instrumentation. Part D.*
391 *Nuclear Tracks and Radiation Measurements*, 14, 203-207.

392

393 Tamura, T., 2012. Beach ridges and prograded beach deposits as environment records.
394 *Earth Science Reviews*, 114, 279-297.

395

396 Thom, B.G., Polach, H.A., Bowman, G.M., 1978. Holocene age structure of coastal sand
397 barriers in New South Wales, Australia: Geography Department Report. Duntroon:
398 University of New South Wales.

399

400 Lauer, J.W., Parker, G., Dietrich, W.E., 2008. Response of the Strickland and Fly River
401 confluence to postglacial sea level rise. *Journal of Geophysical Research*, 113, F1,
402 doi:10.1029/2006JF000626

403

404 West, R.C., Psuty, N.P., Thom, B.G., 1969. The Tabasco Lowlands of Southeastern
405 Mexico. Louisiana State University Press: Coastal Studies Series Number 27.

406 **Figure captions**

407

408 **Figure 1.** Location map of the strand-plain of the Usumacinta and Grijalva rivers in the
409 delta plain of Tabasco and Campeche. In A Current position of the Usumacinta and Grijava
410 rivers in the delta plain and location of blocked-valley lakes. Numbers correspond to
411 archeological sites, 1 = Comacalco; 2 = Palenque; 3 = Balancan and 4 = El Tigre. The
412 topographic data is from ASTER Global DEM of 30 m of resolution, ASTER GDEM is a
413 product of METI and NASA. In B is shown the former delta of Grijalva river at western
414 sector of the delta plain and prior to the formation of the Usumacinta and Grijalva strand-
415 plain (see Fig. 2). Topography extracted from 5m LIDAR DEM produced by INEGI.

416

417 **Figure 2.** Phases of evolution of the strand-plain of the Usumacinta and Grijalva rivers and
418 OSL ages. The inset shows the correlation between OSL ages and the distance of samples
419 from shoreline confirming a markedly progradation of beach-dune ridges from inland
420 towards the sea. The delta plain initiated the aggradation process at ~7 ka evidence by the
421 blocked-valley lakes located 90 km off the shoreline (see Fig. 1A). The satellite images are
422 from Landsat 8 by the NASA) and available in the USGS webpage
423 (<https://earthexplorer.usgs.gov>).

424 Figure 3. Well-preserved beach-dune ridges of the strand-plain of the Usumacinta and
425 Grijalva river in Campeche. In this site, crests over the inundated terrain in the swales
426 allowing the identification of these parallel geomorphological forms. The width of ridges is
427 about 2-3 m and difference of elevation between top of crests and bottom of swales is > 1
428 m.

429

430 Figure 4. Erosive shoreline at SPSP River. Notice that a remaining ridge in the front of the
431 picture is partially destroyed by the effect of the waves.

432

433 **Figure 5.** Progradation rate (m yr⁻¹) and period of formation (years per bar) for different
434 reported strand-plain around the world. The Usumacinta-Grijalva is among the highest
435 progradation rates and shortest periods of bar formation. Data of Tagueman Bay and Grand
436 Traverse Bay by Argyilan et al., (2005); Canaveral Peninsula and Merrit Island by Rink and
437 Forrest, (2005); Grinchen Bay by Murray-Wallace et al., (2002); Skallingen Spit by
438 Aagaard et al., (2007); Phra Thong Island by Brill et al., (2012); New South Wales by
439 Thom et al., (1978) and Apalachicola Barrier by Rink and Lopez, (2010).

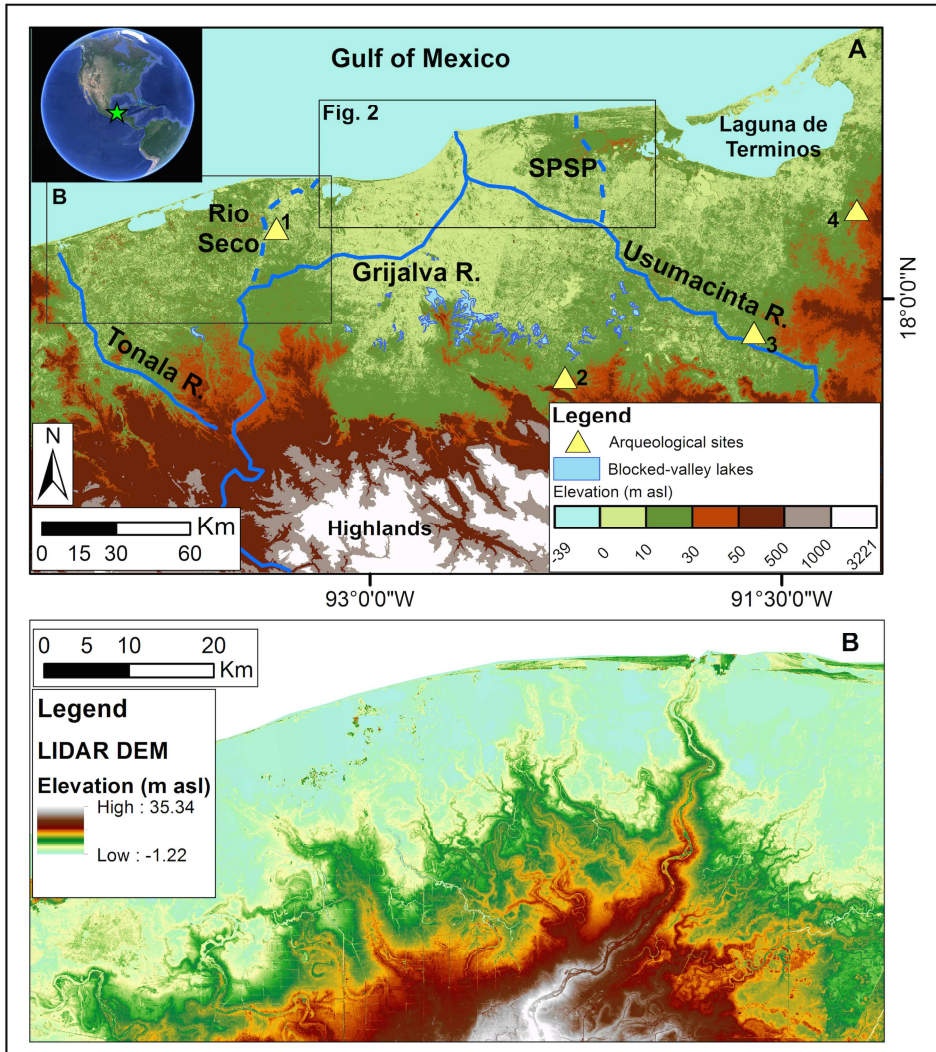
Table 1. List of the age of samples dated for AMS ^{14}C analysis in Beta Analytic Laboratory.

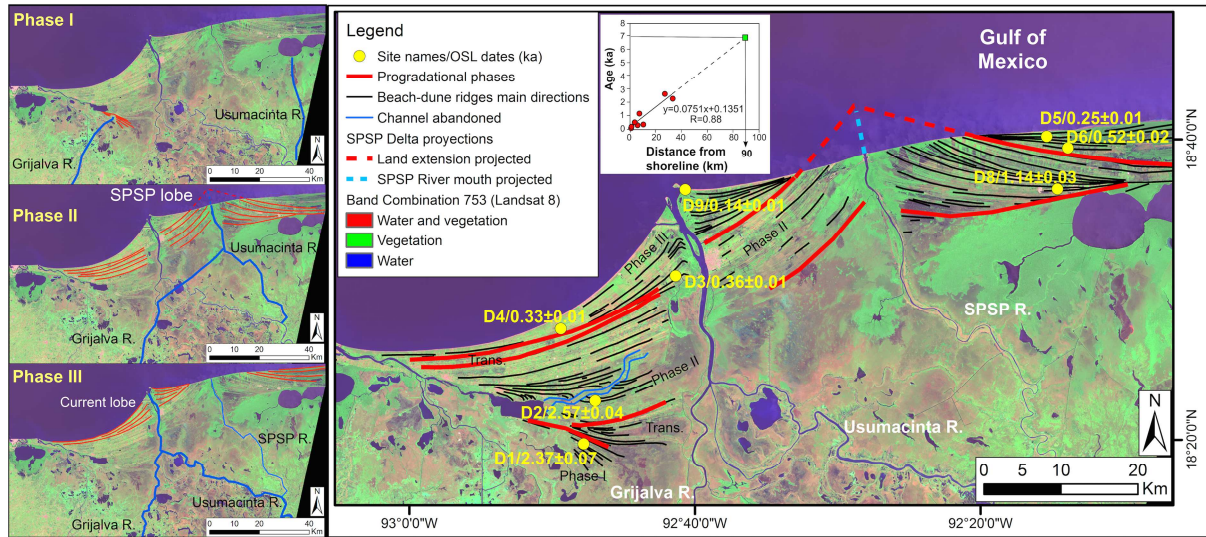
ID	Lab code	Easting	Northing	^{14}C age	Cal. ^{14}C age ^a	Material
D9	Beta - 442567	18°36'40.04395	92°40'40.62489	106.8 +/- 0.3 pMC	Post 0 BP	Plant material
D8	Beta - 442568	18°36'42.32562	92°14'36.39035	210 +/- 130 BP	233 ± 236 BP	Plant material
D3	Beta - 442569	19°30'55.06019	92°41'21.52405	180 +/- 30 BP	180 ± 44 BP	Charred material
D1	Beta - 442570	18°19'44.06024	92°47'48.30420	100.7 +/- 0.3 pMC	Post 0 BP	Organic sediment

^aCalibration using IntCal 13.14C (Reimer et al 2013) using the code "CLAM" (Blaawn 2010) written for R (R Development Core Team 2009).

Table 2. Sample names, location and OSL ages obtained for the eight sites around the strand-plain of the Usumacinta and Grijalva rivers. Errors stated are \pm standard error (weighted standard deviation). Dose rate was estimated from high-resolution gamma spectrometry (using a EG&G Ortec Gamma-X detector) and a thick source beta counting system (Sanderson, 1988). Effective beta and gamma dose rates followed water corrections with grain size attenuation factors of Mejdahl (1979) for K, U, and Th, and including cosmic dose contribution (Prescott and Hutton, 1994). Equivalent doses were performed in grains of quartz using a Risø DA-15 automatic reader and following a single aliquot regeneration (SAR) protocol (Murray and Wintle, 2000) (For further details on the analytical procedures consult the laboratory report of Kinnaird et al., 2016).

ID	Lab code	Location and Elevation			OSL ages	
Field no.	SUTL no.	Northing	Easting	m asl	Years / ka	Calendar years
D1	2842	18° 19'44.06024	92° 47'48.30420	7	2.37 \pm 0.07 (0.38)	-360 \pm 70 (380)
D2	2843	18° 22'35.39771	92° 46'59.04204	1.57	2.57 \pm 0.04 (0.30)	-560 \pm 40 (300)
D3	2844	19° 30'55.06019	92° 41'21.52405	2.88	0.36 \pm 0.01 (0.04)	1660 \pm 15 (40)
D4	2845	18° 27'23.88197	92° 49'24.17609	0.78	0.33 \pm 0.01 (0.04)	1685 \pm 10 (40)
D5	2846	18° 40'11.78538	92° 15'21.74478	3.2	0.25 \pm 0.01 (0.01)	1770 \pm 10 (15)
D6	2847	18° 39'26.48189	92° 13'52.57510	3.5	0.52 \pm 0.02 (0.06)	1500 \pm 20 (60)
D8	2849	18° 36'42.32562	92° 14'36.39035	0	1.14 \pm 0.03 (0.07)	875 \pm 30 (70)
D9	2850	18° 36'40.04395	92° 40'40.62489	0	0.14 \pm 0.01 (0.06)	1880 \pm 5 (60)



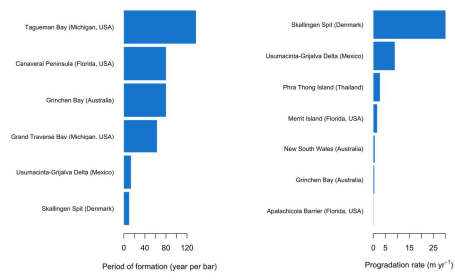




ACCEPTED MANUSCRIPT



ACCEPTED MANUSCRIPT



ACCEPTED MANUSCRIPT

- A robust OSL geochronological record for the strand-plain of Tabasco and Campeche
- Different phases of evolution of the strand-plain of Usumacinta and Grijalva rivers
- Aggradation of the coastal plain of Tabasco and Campeche initiated ~7 ka

ACCEPTED MANUSCRIPT